



Analysis of Height Stability of Object Points of Monolithic Construction

Slavomír LABANT¹⁾*, Hana STAŇKOVÁ²⁾, Pavel ŠUSTEK⁴⁾, Lubomír LEICHER⁵⁾, Tereza JADVIŠČOKOVÁ⁶⁾, Martina HULANOVÁ⁷⁾, Vladimír BRŮNA⁸⁾, Štefan RÁKAY³⁾

¹⁾ Technical University of Košice, Faculty of Mining, Ecology, Process control and Geotechnologies, Institute of Geodesy, Cartography and GIS, Letná 9, 04001, Košice, Slovak Republic; ORCID <https://orcid.org/0000-0002-0666-4268>

²⁾ VŠB - Technical University of Ostrava, Faculty of Mining and Geology, Department of Geodesy and Mine Surveying, 17. listopadu 15, Ostrava - Poruba, 708 00, Czech Republic; ORCID <https://orcid.org/0000-0003-0013-3666>

³⁾ Land and Forestry Department of the Kosice District Office, Hroncova 13, SK 04200 Kosice, Slovak Republic; ORCID <https://orcid.org/0000-0002-0583-9783>

⁴⁾ VŠB - Technical University of Ostrava, Faculty of Mining and Geology, Department of Geodesy and Mine Surveying, 17. listopadu 15, Ostrava - Poruba, 708 00, Czech Republic; ORCID <https://orcid.org/0009-0003-7930-9931>

⁵⁾ VŠB - Technical University of Ostrava, Faculty of Mining and Geology, Department of Geodesy and Mine Surveying, 17. listopadu 15, Ostrava - Poruba, 708 00, Czech Republic; ORCID <https://orcid.org/0009-0008-7742-1176>

⁶⁾ VŠB - Technical University of Ostrava, Faculty of Mining and Geology, Department of Geodesy and Mine Surveying, 17. listopadu 15, Ostrava - Poruba, 708 00, Czech Republic; ORCID <https://orcid.org/0009-0002-3739-996X>

⁷⁾ VŠB - Technical University of Ostrava, Faculty of Mining and Geology, Department of Geodesy and Mine Surveying, 17. listopadu 15, Ostrava - Poruba, 708 00, Czech Republic; ORCID <https://orcid.org/0009-0008-7333-717X>

⁸⁾ VŠB - Technical University of Ostrava, Faculty of Mining and Geology, Department of Geodesy and Mine Surveying, 17. listopadu 15, Ostrava - Poruba, 708 00, Czech Republic; ORCID <https://orcid.org/0000-0003-2789-860X>

* Corresponding author: slavomir.labant@tuke.sk

<http://doi.org/10.29227/IM-2024-01-87>

Submission date: 10-05-2024 | Review date: 03-06-2024

Abstract

Geodetic measurements aim to monitor the behaviour of objects and prevent various degrees of non-functionality or destruction. By measuring vertical movements, the height stability of the monolithic building is monitored concerning the previous stages of measurement. The measurements were carried out using a digital levelling instrument, the Leica DNA03 and invar code bars GPCL2 with a length of 2 m. The object points were mainly stabilized in the supporting structure of the building, but stabilization in the ceiling was also necessary in problematic areas. Object points in the ceiling were measured using a special metal hanging holder for levelling rods. After the initial verification of the measured elevations, and whether they meet the accuracy criteria, processing followed by the application of the Gauss-Markov model based on the method of least squares corrections. The estimates of the unknown parameters from the stage measurements were used to calculate the height differences of the observed points, which characterize the behaviour of the monolithic object. Significant height changes were detected based on the accuracy of the estimated heights, determining whether they represented significant drops or just an accumulation of measurement errors. The height changes of the object points were graphically visualized in 1D as time series of decline and in 2D as isolines of vertical displacements based on the floor plan of the monolithic building.

Keywords: monolithic construction, levelling, stability monitoring, height changes, isolines of movements

1. Introduction

With the civilization's development, more complex constructions began to be built and more interventions by man into nature took place. Everything that is on the earth's surface, but also under it, is in constant motion. This is because different forces act on objects and their structures, which want to achieve mutual balance. Objects change their shape after some time and that negatively affects their functionality, and also their surroundings. Every change in the object's position and geometry (shape and dimensions) is a consequence of the action of various deformation forces. They are created by the action of various physical, chemical, biological, and other processes that affect the object and its surroundings. The effects of these forces cause internal as well as external changes, which geodesy and other measurement technologies can characterize and quantify with their

procedures and methods [9]. New and atypical building structures must be regularly geodetically monitored to prevent deformations in them. Horizontal, vertical, or even spatial changes occur on construction objects. The horizontal movement in the Cartesian system is given by the components ΔX and ΔY . A vertical displacement is either a rise or a fall and is denoted as ΔZ or Δh . When measuring the deformations of engineering structures (bridges, dams, tunnels, etc.), all three components are usually measured ΔX , ΔY , ΔZ and their 3D changes [7].

2. Determining movements of construction objects

As a result of the action of deformation forces, various horizontal and vertical displacements of the entire object or only parts of the object or various tilting of the object, shape changes of individual constructions, foundations and

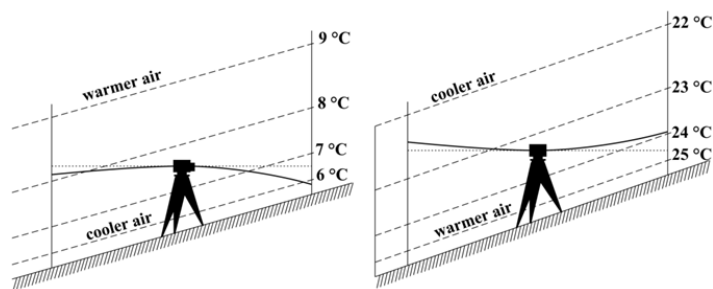


Fig. 1. Levelling refraction depending on the temperature of the air layers [2]

Rys. 1. Załamanie niwelacyjne w zależności od temperatury warstw powietrza [2]



Fig. 2. The building of the University Science Park Technicom

Rys. 2. Budynek Uniwersyteckiego Parku Naukowego Technicom

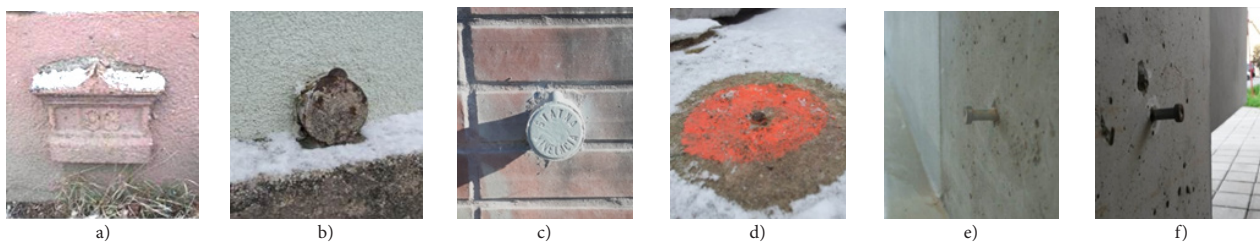


Fig. 3. Reference points no. 193, 194, 195, 5001, and object points in the Technicom interior

Rys. 3. Nr punktów referencyjnych 193, 194, 195, 5001 oraz punkty obiektowe we wnętrzu Technicomu

subsoil of the object occur. When the soil is loaded with a construction object, it compresses and settles. For example, gravel and sand settle only a few millimetres, while on other very compressible soils, they may settle up to several decimetres. It is dangerous if the object sits unevenly, resulting in various cracks forming on the construction object that grows larger over time [7]. The purpose of measuring displacements and deformations of construction objects according to is [14]:

- to obtain materials for assessing the effects of construction on the foundation soil,
- to compare actual shift values with expected shift values in projects,
- and to monitor the condition, functionality, reliability, and safety of construction objects.

To monitor the stability of the construction object, a displacement measurement project will be developed. In the measurement project, the following shall be stated in particular [14]: the purpose and meaning of the measurement, data on the properties of the foundation soil, construction data, expected displacement values, required measurement accuracy, measurement methods, location of object and reference points, schedule for staged measurements, method of processing measurement results and their interpretation.

Measurement of vertical displacements and deformations is most often performed by geometric levelling, trigonometric method, photogrammetric methods, or physical methods [7]. Geometric levelling from the centre is the fastest, most used and most accurate method of measuring height differences [1]. High-precision levelling or precision levelling is most often used to measure vertical displacements. For demanding tasks, e.g. movements of the earth's crust, special-precision levelling is used [7]. For such tasks, a point field is also needed, which consists of:

- reference points – their location is chosen in places that are not affected by construction activity and deformation forces [14]. When stabilizing the reference points, the groundwater level and the depth of soil freezing (0.3 to 1.3 m) must also be considered [7]. When creating new reference points, the so-called heavy stabilization is firmly connected to the bed-rock (concrete pillars and blocks) [9].
- object (observed) points – their position, density, number, and location of observed points are chosen to determine displacements and deformations of the observed building object. According to the project, they are stabilized on the monitored object with levelling marks, which are firmly inserted into the object in advance before the start of the measurement [14].

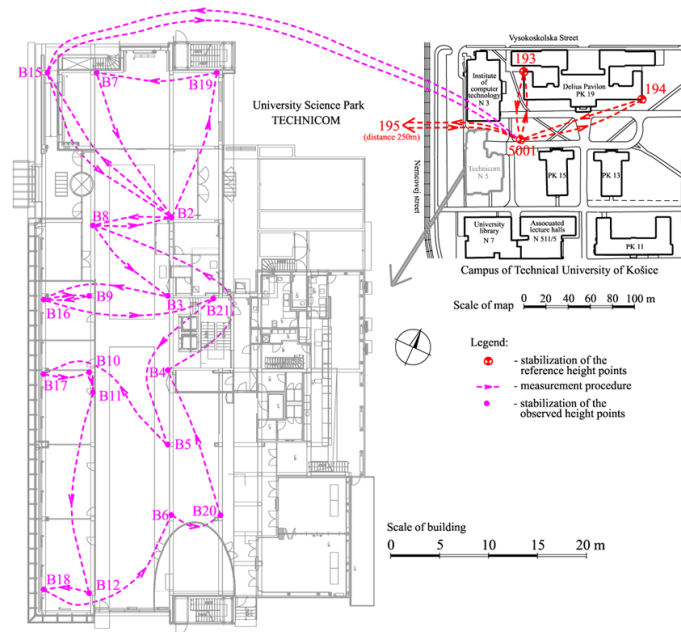


Fig. 4. Location sketch and measurement procedure of reference and observed height points
Rys. 4. Szkic lokalizacji i procedura pomiaru punktów odniesienia i obserwowanych wysokości

In Slovakia, the points of the geodetic foundations are also the points of the state levelling network (SLN). SLN points have determined exact normal heights according to Molodensky in the valid national implementation of the Baltic Vertical Datum – After Adjustment (BVD-AA) (1957) with EPSG code 8357 [15]. Altitudes in SLN refer to the mean level of the Baltic Sea in Kronstadt. Levelling marks are stabilized in permanent objects where it is assumed that the object is height stable (massive walls of public buildings, bridge piers, etc.). To stabilize object points, pin (on the object) or nail (into a solid foundation) marks are used. Pin levelling marks are firmly set into the object at a height of approx. 0.5 m above the ground with free space above the mark for the vertical position of the batten [10]. The problem arises if the pin mark is on a building that has been thermally insulated and left a small "window" around the pin mark.

The air layers above the earth's surface are not equally dense, and when a light beam passes through them, the beam is refracted, and refraction (curvature of the light beam) occurs (Fig. 1). According to [2], the transition of the beam between the layers is smooth and curved. The main source of heat is solar radiation, of which 42% is reflected, 15% is absorbed by the atmosphere and 43% falls on the earth's surface. Light beams pass through clean air and the air is heated from the surface of the soil. Due to the unevenness and roughness of the soil, masses of superheated air are created, which later rise in the form of bubbles in swirling movements. Cool air currents descend between them to warm up. This creates air circulation, where the layers are overheated at the bottom, air currents of different temperatures fall and rise in the middle, and the rising currents rotate at the top.

Only precise digital levelling is used for measurement in the SLN. According to [13] such measurements are subject to accuracy requirements:

a) the deviation ρ in elevation between two levelling points (double-run levelling) must not exceed the value of the extreme deviation which is:

- in 1st-order SLN $\rho \leq \rho_{1,\max} = 1.50\sqrt{R}$ [mm], (1)
- in 2nd-order SLN $\rho \leq \rho_{II,\max} = 2.25\sqrt{R}$ [mm], (2)

b) the standard deviation for 1 km double-run levelling:

$$m_0 = \frac{1}{2} \sqrt{\frac{1}{n_R} \sum_{i=1}^n \frac{\rho_i^2}{R}} \text{ [mm]}, \quad (3)$$

c) extreme deviation of the standard deviation for 1 km double-run levelling :

- for 1st-order SLN $m_0 \leq m_{0_I,\max} = 0.40 + \sqrt{\frac{1}{n_R}}$ [mm], (4)

- for 2nd-order SLN $m_0 \leq m_{0_II,\max} = 0.45 + \sqrt{\frac{1}{n_R}}$ [mm], (5)

d) the identity of the connection points must be verified according to the topography and by checking the elevation, the deviations between the original and the control elevation must not exceed the extreme deviation:

- for a section of the levelling network of the 1st-order: $2.00 + 1.5\sqrt{R}$ [mm], (6)
- for a section of the levelling network of the 2nd-order: $2.00 + 2.25\sqrt{R}$ [mm], (7)

where n_R is a number of sections, R is a haul length in km and ρ is deviation in elevation.

3. Materials and methods

Stability monitoring was carried out in stages at the building of the University Science Park (USP) Technicom (Fig. 2). This monolithic structure is located on the TUKE campus and has been geodetically monitored since 2016. During construction, the horizontality of individual floors was also determined using trigonometric levelling [8]. The USP Technicom building began to be built in 2013 in cooperation with the Technical University in Košice, the University of Prešov in Prešov and the University of Pavel Jozef Šafárik in Košice. USP Technicom according to [16]:

- creates an ecosystem for the acceleration of technological transfer, innovation, and business support,

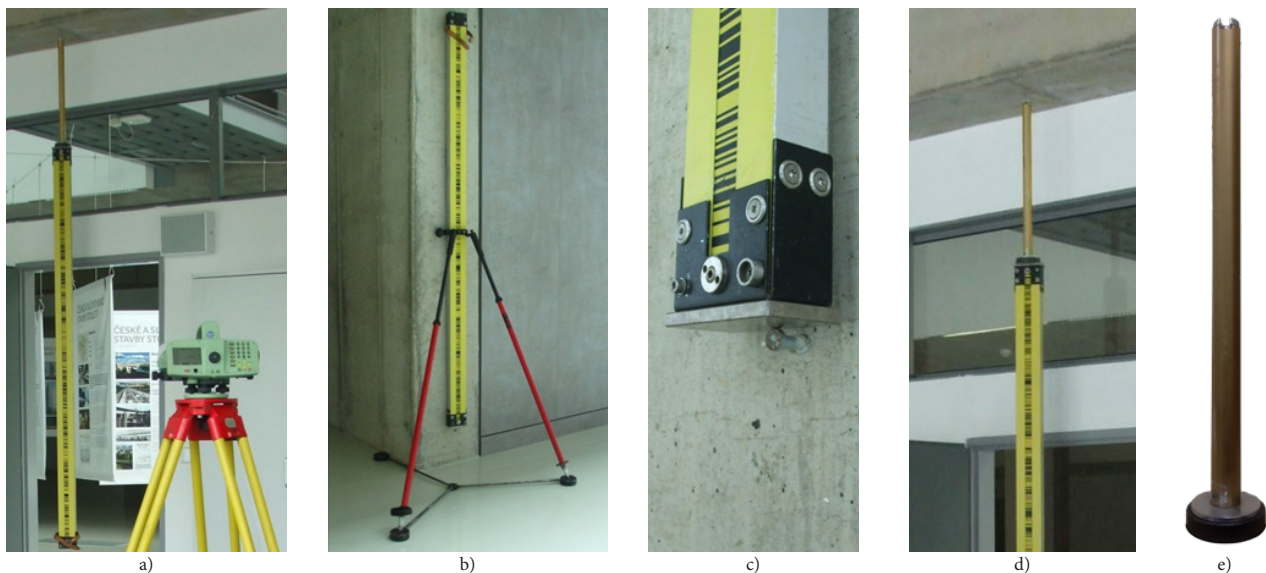


Fig. 5. Position of the invar bar code rod from the ceiling and on the point
 Rys. 5. Położenie inwarowego pręta kodu kreskowego od sufitu i na punkcie

- provides space for the support of applied research and development,
- ensures the transfer of research and development results into economic and social practice and supports the creation and development of businesses,
- provides an incubation environment for the creation and development of innovative startup and spin-off companies.

Before commencing the initial stage of measurement, a reconnaissance of the existing point field surrounding the construction object and a proposal for the location of the observed points according to the designer's specifications was conducted. Within the vicinity of the constructed building, four reference height points were selected: 193, 194, 195, and 5001. Points 193 and 194 are secured by pin levelling marks in the foundations of the Delius Pavilion building (Fig. 3 a, b). A pin levelling mark anchors point 195 within the foundations of the Košice-Okolie District Office building (Fig. 3 c). Additionally, a steel geodetic nail embedded in the concrete block of the old foundations serves as point number 5001 (Fig. 3 d). These four reference points serve to check each other if any of them move and also serve to connect observed points by the levelling loop. The height connection to the Baltic Vertical Datum – After Adjustment was established using point no. 193 (Fig. 3 a) with its altitude denoted as $H_{193} = 213.99480$ m. The location and distribution of reference height points are illustrated in the situation sketch (Fig. 4 right). The observed points, after consultation with the designer, were secured within the supporting structure of the monolithic building. At the selected locations were anchored observed points B2 to B21 using steel measuring pins (Fig. 3 e, f). The position and distribution of points are outlined in the sketch (Fig. 4 left).

The determination of the heights of reference and observed points was carried out by the conditions established for high-precise levelling. For measurement used: the digital levelling instrument Leica DNA03 (Fig. 5 a), heavy wooden tripod Leica GST20-9 (Fig. 5 a), floor mat for the tripod (Fig.

5 b), two levelling invar bar code rod type GPCL2 (length 2 m) with a precise spirit level (Fig. 5 b), bipods for levelling rods (Fig. 5 b) and levelling pads. The Leica DNA03 is used for very accurate determination of heights and using an invar batten with parameters $\Delta L = \pm 0.02 \text{ mm} + L \cdot 2 \cdot 10^{-5}$, and $\alpha_r < 1 \text{ ppm}/^\circ\text{C}$ achieves a standard deviation for 1 km double-run levelling $\sigma_{\text{km}} = \pm 0.3 \text{ mm}$ [12]. The resolution of the height reading on the invar bar code is 0.01 mm. The standard error in automatic measuring in laboratory conditions for the levelling measurement instrument of the Leica DNA03 with a 2-m invar bar code of the levelling rod was determined to be $\pm 1.3 \mu\text{m}$ [4]. The Leica DNA03 instrument with battery weighs 2.4 kg, the heavy wooden tripod GST20-9 with extendable legs weighs 6.4 kg, and the 2 m long GPCL2 levelling bars weigh 4.2 kg. The levelling instrument needs visibility of at least 38 cm section of the levelling batten for 20 m without disturbing influences (shadow, vegetation). Before the measurement itself, the main axis condition of the levelling instrument was verified by the most accurate Nábauer procedure, which eliminates the effects of refraction and curvature of the Earth [11].

Levelling measurements were conducted in five stages: the 0th stage in March 2016, the 1st stage in June 2016, the 2nd stage in July 2017, the 3rd stage in June 2018, and the 4th stage in May 2019. These stage measurements were then divided into three levelling sections or moves. The first levelling section involved measurements through reference points 193, 194, 195, and 5001 (Fig. 4 right). The second levelling section extended from point 5001 through B15 to point B2, situated on the ground floor inside the building (Fig. 4 left). Within the building, on the ground floor, the third closed levelling loop was measured across 17 points, spanning from point B2 to B21. A digital levelling instrument (Fig. 5 a) was mounted on a tripod and placed on a special pad to prevent damage to the floor (Fig. 5 b). Most points were secured in the pillars of the monolithic structure using steel measuring pins, allowing for the levelling invar bar code rod to be placed without difficulty (Fig. 5 b, c). The rods were aligned vertically using a spirit-level vial and supported by a bipod. For points an-

Tab. 1. Assessment of the accuracy of measurement of levelling sections and loops

Tab. 1. Ocena dokładności pomiarów odcinków i pętli niwelacyjnych

Stage	Year/Month	1st levelling section			2nd levelling section			3rd levelling loop		
		ρ_1 [mm]	$\rho_{1,max}$ [mm]	test OK/NO	ρ_2 [mm]	$\rho_{2,max}$ [mm]	test OK/NO	m_0 [mm]	$m_{0,max}$ [mm]	test OK/NO
0.	2016/03	0.17	1.11	OK	0.13	0.44	OK	0.15	0.64	OK
1.	2016/06	0.19	1.10	OK	0.06	0.43	OK	0.35	0.64	OK
2.	2017/07	-0.15	1.09	OK	-0.10	0.44	OK	0.02	0.64	OK
3.	2018/06	-0.18	1.11	OK	0.06	0.45	OK	0.21	0.64	OK
4.	2019/05	0.25	1.12	OK	0.03	0.44	OK	0.16	0.64	OK

chored in the ceiling, a special magnetic hanger was utilized to suspend the invar bar code rod from above (Fig. 5 a, d, e, point B11). As the network of observed points was planned in consultation with the designer before the construction of internal partitions, certain points in subsequent stages could not be observed due to changes in construction and were consequently omitted entirely.

4. Processing of measured data

Measured values of levelling measurements Δh to determine the heights of the observed points h , were processed using the Gauss-Markov model with the full rank of matrix A . It is about the application of MLS (method of least squares) as a conventional adjustment method. Point no. 193 was used as a reference point for the datum network fixation and its height was not changed by the processing. For the given network to be adjusted and in the result to determine the best possible estimates of the heights of the determined points, the condition of measurement redundancy (overdetermination of the network) must apply in the case of this adjustment: $r = n - k$.

The most used method for adjusting the height net is the Gauss-Markov model (GMM) with the full rank of the matrix A of the form:

$$\begin{aligned} \mathbf{v} &= \mathbf{A}d\hat{\mathbf{h}} - d\Delta\mathbf{h} = \mathbf{A}(\hat{\mathbf{h}} - \mathbf{h}^\circ) - (\Delta\mathbf{h} - \Delta\mathbf{h}^\circ), & \text{- funkcjonal part,} \\ \Sigma_{\Delta\mathbf{h}} &= s_0^2 \mathbf{Q}_{\Delta\mathbf{h}}, & \text{- stochastic part,} \end{aligned} \quad (8)$$

where \mathbf{v} represents the correction (residuals) vector of the observed quantities Δh , $d\Delta\mathbf{h} = \Delta\mathbf{h} - \Delta\mathbf{h}^\circ$ is the vector of reduced elevations, $d\hat{\mathbf{h}} = \hat{\mathbf{h}} - \mathbf{h}^\circ$ is the vector of the estimates complements of determined heights and A is the configuration matrix (matrix of partial derivatives).

The adjusting procedure of measured levelling elevations between points and determination of estimates of unknown point's height consists of the following steps:

1. Arrangement of input data:

- vector of measured elevations Δh among all points with a number n ,
- vector of approximate point heights h° with number k was determined using the reference height of point 193 and the measured elevations Δh ,
- cofactor matrix of measured elevations $\mathbf{Q}_{\Delta\mathbf{h}}$ characterizes the quality of elevation Δh , where used σ^2 is the a priori variance of the measurement method depending on the choice of weights.

2. Creation of model equations:

- vector of the approximate elevations Δh° is determined from the difference in the approximate heights of the points h° ,
- vector of the reduced elevations $d\Delta\mathbf{h}$ is determined from the relationship $\Delta\mathbf{h} - \Delta\mathbf{h}^\circ$.

3. Creation of configuration matrix:

- design matrix A characterizes the tensile structure of the connection of points in the network and there are determined the partial derivatives of the functions of the approximate elevations Δh° according to approximate heights h° .

4. Calculation of estimates:

- vector of estimates of determined heights $\hat{\mathbf{h}}$ is obtained by the sum of the vector complements of the height estimates $d\hat{\mathbf{h}}$ and the vector of approximate heights h° .

- vector of estimates of measured elevations $\hat{\Delta\mathbf{h}}$ is obtained by the sum of the vector of measured elevations $\Delta\mathbf{h}$ and vector of residuals \mathbf{v} .

5. Expression of the accuracy of the parameters of the levelling network:

- unit a posteriori variance s_0^2 is determined based on the minimization condition of MLS,
- the covariance matrix of height estimates $\Sigma_{\hat{\mathbf{h}}}$ contains the main diagonal empirical variances of the heights of individual points $\sigma_{\hat{h}_j}$,
- the covariance matrix of elevation estimates $\Sigma_{\hat{\Delta\mathbf{h}}}$ contains on the main diagonal the empirical variances of the elevation $\sigma_{\Delta\hat{h}_{j,j+1}}$ between the measured points.

The processing of the measured values was carried out by software, and after that, it was verified whether the measurements in individual stages were carried out at the same level of accuracy. This was done based on statistical testing with Fisher's test [9], where the test criterion T is determined by the proportion of unit posterior variances $s_{(i)}^2$ from both stages, which was compared to the critical value F determined at the significance level α and the number of redundant measurements from both stages $f^{(i)}$, $f^{(i+1)}$:

$$T = \frac{s_{(i+1)}^2}{s_{(i)}^2} \approx F(\alpha, f^{(i)}, f^{(i+1)}) \quad (9)$$

In this case $T < F$ it is possible to determine the significance of the height differences of the observed points between individual stages, which consisted according to [6] of:

- estimates of determined heights of points obtained in stages $t^{(i)}$ and $t^{(i+1)}$ were calculated the height differences of the observed points of the monolithic building $d\hat{h}_j^{(i,i+1)}$ according to the relationship:

$$d\hat{h}_j^{(i,i+1)} = \hat{h}_j^{(i+1)} - \hat{h}_j^{(i)} \quad (10)$$

- variances of estimates of point heights obtained in stages $t^{(i)}$ and $t^{(i+1)}$ were calculated variance values of height differences $\sigma_{d\hat{h}_j^{(i,i+1)}}^2$ according to the relationship:

$$\sigma_{d\hat{h}_j^{(i,i+1)}}^2 = \sigma_{\hat{h}_j^{(i)}}^2 + \sigma_{\hat{h}_j^{(i+1)}}^2 \quad (11)$$

Tab. 2. Estimates of the parameters for all stages of monolithic building stability investigation
 Tab. 2. Oszacowania parametrów dla wszystkich etapów badania stateczności budynku monolitycznego

Point	0th measurement stage 2016/03			1st measurement stage 2016/06			2nd measurement stage 2017/07			3rd measurement stage 2018/06			4th measurement stage 2019/05					
	$\hat{h}^{(0)}$	$\sigma_{\hat{h}}^{(0)}$	** Type	$\hat{h}^{(1)}$	$\sigma_{\hat{h}}^{(1)}$	Δh	$\hat{h}^{(2)}$	$\sigma_{\hat{h}}^{(2)}$	Δh	$\hat{h}^{(3)}$	$\sigma_{\hat{h}}^{(3)}$	Δh	$\hat{h}^{(4)}$	$\sigma_{\hat{h}}^{(4)}$	Δh			
	[m]	[mm]		[m]	[mm]	(01)	[m]	[mm]	(12) (02)	[m]	[mm]	(23) (03)	[m]	[mm]	(34) (04)			
Reference points:																		
193	213.99480	0.00	LP	213.99480	0.00	0.00	213.99480	0.00	0.00	0.00	213.99480	0.03	0.00	0.00	213.99480	0.00	0.00	0.00
194	214.06152	0.02	LP	214.06150	0.05	-0.02	214.05872	0.10	-2.78*	-2.80	214.05876	0.08	0.04	-2.76	214.05872	0.09	-0.04	-2.80
195	214.29701	0.03	LP	214.29696	0.04	-0.05	214.29692	0.05	-0.04	-0.09	214.29686	0.06	-0.06	-0.15	214.29682	0.05	-0.04	-0.19
5001	213.28992	0.01	GN	213.28994	0.03	0.02	213.29004	0.06	0.10	0.12	213.29010	0.05	0.06	0.18	213.29012	0.03	0.02	0.20
Observed points:																		
B2	214.03935	0.05	SMP	214.03904	0.05	-0.31	214.03832	0.11	-0.72	-1.03	214.03750	0.08	-0.82	-1.85	214.03686	0.07	-0.64	-2.49
B3	214.02232	0.09	SMP	214.02218	0.13	-0.14	214.02146	0.12	-0.72	-0.86	214.02098	0.09	-0.48	-1.34	214.02022	0.08	-0.76	-2.10
B4	214.06471	0.10	SMP	214.06463	0.13	-0.08	214.06401	0.15	-0.62	-0.70	214.06350	0.12	-0.51	-1.21	214.06279	0.08	-0.71	-1.92
B5	214.06444	0.10	SMP	214.06427	0.18	-0.17	214.06355	0.17	-0.72	-0.89	214.06301	0.14	-0.54	-1.43	214.06240	0.09	-0.61	-2.04
B6	214.07217	0.10	SMP	214.07202	0.15	-0.15	214.07135	0.17	-0.67	-0.82	214.07057	0.14	-0.78	-1.60	214.06997	0.09	-0.60	-2.20
B7	214.13667	0.11	SMP	214.13651	0.11	-0.16	214.13584	0.12	-0.67	-0.83	214.13506	0.09	-0.78	-1.61	point is inaccessible			
B8	214.01755	0.07	SMP	214.01739	0.08	-0.16	214.01685	0.13	-0.54	-0.70	214.01600	0.10	-0.85	-1.55	214.01536	0.07	-0.64	-2.19
B9	214.00232	0.08	SMP	214.00247	0.14	0.15	214.00194	0.15	-0.53	-0.38	214.00115	0.12	-0.79	-1.17	214.00058	0.08	-0.57	-1.74
B10	214.01690	0.09	SMP	214.01636	0.18	-0.54	214.01545	0.17	-0.91	-1.45	214.01444	0.14	-1.01	-2.46	214.01342	0.09	-1.02	-3.48
B11	216.58603	0.10	SMP	216.58584	0.17	-0.39	216.58531	0.19	-0.84	-1.23	216.58446	0.17	-0.85	-2.08	216.58351	0.08	-0.95	-3.03
B12	213.99821	0.10	SMP	213.99814	0.18	-0.07	213.99680	0.19	-1.34	-1.41	213.99485	0.16	-1.95	-3.36	213.99339	0.09	-1.46	-4.82
B15	213.98742	0.05	SMP	213.98720	0.05	-0.22	213.98640	0.12	-0.80	-1.02	213.98578	0.09	-0.62	-1.64	213.98475	0.04	-1.03	-2.67
B16	214.01061	0.08	SMP	214.01067	0.14	0.06	214.00990	0.15	-0.77	-0.71	214.00912	0.12	-0.78	-1.49	214.00856	0.08	-0.56	-2.05
B17	214.05708	0.09	SMP	214.05694	0.18	-0.14	214.05641	0.17	-0.53	-0.67	214.05586	0.14	-0.55	-1.22	214.05553	0.09	-0.33	-1.55
B18	213.99836	0.10	SMP	213.99816	0.17	-0.20	213.99752	0.19	-0.64	-0.84	213.99684	0.16	-0.68	-1.52	213.99613	0.09	-0.71	-2.23
B19	214.03094	0.15	SMP	214.03106	0.11	0.12	214.03038	0.12	-0.68	-0.56	214.02962	0.09	-0.76	-1.32	point is inaccessible			
B20	214.01220	0.10	SMP	214.01205	0.15	-0.15	214.01145	0.15	-0.60	-0.75	214.01046	0.12	-0.99	-1.74	214.00967	0.09	-0.79	-2.53
B21	214.18229	0.10	SMP	214.18241	0.16	0.12	point was destroyed											

**Type: LP - levelling pin on building; GN - geodetic nail; SMP - steel measuring pin; -2.78* - facade repair

3) the critical value $dh_{j_{ku}}^{(i,j+1)}$ for the difference in height estimates $\hat{dh}_j^{(i,j+1)}$ of the observed point was calculated according to the relationship:

$$\hat{dh}_{j_{ku}}^{(i,j+1)} = t \cdot \sigma_{\hat{dh}_j^{(i,j+1)}}^2, \quad (12)$$

where t is confidence coefficient with value t = 2.5 according to the chosen significance level $\alpha = 0.01$ with probability p = 98,8 %,

4) comparison of the height difference of the relevant observed point $\hat{h}^{(i,j+1)}$ and its relevant critical value $dh_{j_{ku}}^{(i,j+1)}$ it is possible to conclude the significance of the height difference between stages $t^{(i)}$ and $t^{(i+1)}$ if this applies:

$$\left| \hat{dh}_j^{(i,j+1)} \right| < dh_{j_{ku}}^{(i,j+1)}, \quad (13)$$

it is possible to conclude that the point is stable, and the height difference is the effect of the accumulation of measurement errors, but in the case of:

$$\left| \hat{dh}_j^{(i,j+1)} \right| \geq dh_{j_{ku}}^{(i,j+1)}, \quad (14)$$

it is possible to conclude that the point is unstable, and the corresponding height difference is significant.

5. Results

After the completion of the levelling measurements in the individual stages of monitoring the height stability of the monolithic building, the data was pre-processed and verified whether the measurements met the required precision. The deviations and the standard deviation for 1 km double-run levelling of the individual stages (Tab. 1) met the required criteria according to equations 1–7 [13].

Estimation of the heights of the observed points \hat{h} and their standard deviations was performed using the Gauss-Markov model based on the MLS, where it was necessary to choose the measurement weight. If the weight of the levelling elevation is dependent on:

- the length of the section and the accuracy of the instrument used, then the measurement variance can be $\sigma_{km} = \pm 0.3$ mm for 1 km, and σ_0 is simple average of all σ_i value,
- the number of levelling instrument positions, then $\sigma = \pm 0.018$ mm for one instrument position, considering that with the average sight length approx. 30 m, possibly for one km approx. $1000m/(2 \cdot 30m) \approx 17$ instrument positions, so $\sigma_{km} = \pm 0.3$ mm/km is divided by 17 instrument positions/km will be assigned ± 0.018 mm on the one instrument positions [3], [5].

The measurement weights were used in the calculation depending on the length of the levelling sections and the accuracy of the instrument. If the weights of the measurements were used as the number of levelling instrument positions, the same measurement weights would be obtained, since in the interior only one instrument position was used between adjacent height points. That is, at the scales p = 1 the same corrections would thus be obtained v and $\sigma_{\Delta \hat{h}_{j,j+1}}$. The numerical values of height estimates and their standard deviations of all observed points, including their height differences $\mathbf{dh}^{(i,j+1)} = \hat{h}^{(i+1)} - \hat{h}^{(i)}$ between the observed stages i and i+1, are arranged in Tab. 2. Over time, it happened that the points were unavailable or destroyed.

After the processing of the current stage of levelling measurements for tracking height changes, it was verified by the Fisher test from equation (9) whether the compared stages are at the same accuracy level. In the case of a positive result of the

Tab. 3. Verification of the stability of the observed points based on the previous stage
 Tab. 3. Weryfikacja stabilności obserwowanych punktów na podstawie poprzedniego etapu

Point	Measur. stages 0-1 2016/03 – 2016/06				Measur. stages 1-2 2016/06 – 2017/07				Measur. stages 2-3 2017/07 – 2018/06				Measur. stages 3-4: 2018/06 – 2019/05			
	$\hat{dh}^{(01)}$ [mm]	$\sigma_{\hat{dh}^{(01)}}^2$ [mm]	$dh_{krit}^{(01)}$ [mm]	sig	$\hat{dh}^{(12)}$ [mm]	$\sigma_{\hat{dh}^{(12)}}^2$ [mm]	$dh_{krit}^{(12)}$ [mm]	sig	$\hat{dh}^{(23)}$ [mm]	$\sigma_{\hat{dh}^{(23)}}^2$ [mm]	$dh_{krit}^{(23)}$ [mm]	sig	$\hat{dh}^{(34)}$ [mm]	$\sigma_{\hat{dh}^{(34)}}^2$ [mm]	$dh_{krit}^{(34)}$ [mm]	sig
Reference points:																
194	-0.02	0.05	0.13		-2.78*	0.11	0.28	s	0.04	0.13	0.32		-0.04	0.12	0.30	
195	-0.05	0.05	0.13		-0.04	0.06	0.16		-0.06	0.08	0.20		-0.04	0.08	0.20	
5001	0.02	0.03	0.08		0.10	0.07	0.17		0.06	0.08	0.20		0.02	0.06	0.15	
Observed points:																
B2	-0.31	0.07	0.18	s	-0.72	0.12	0.30	s	-0.82	0.14	0.34	s	-0.64	0.11	0.27	s
B3	-0.14	0.16	0.40		-0.72	0.18	0.44	s	-0.48	0.15	0.38	s	-0.76	0.12	0.29	s
B4	-0.08	0.16	0.41		-0.62	0.20	0.50	s	-0.51	0.19	0.48	s	-0.71	0.15	0.36	s
B5	-0.17	0.21	0.51		-0.72	0.25	0.62	s	-0.54	0.22	0.55		-0.61	0.17	0.42	s
B6	-0.15	0.18	0.45		-0.67	0.23	0.57	s	-0.78	0.22	0.55	s	-0.60	0.16	0.41	s
B7	-0.16	0.16	0.39		-0.67	0.16	0.41	s	-0.78	0.15	0.38	s				
B8	-0.16	0.11	0.27		-0.54	0.15	0.38	s	-0.85	0.16	0.41	s	-0.64	0.12	0.31	s
B9	0.15	0.16	0.40		-0.53	0.21	0.51	s	-0.79	0.19	0.48	s	-0.57	0.14	0.36	s
B10	-0.54	0.20	0.50	s	-0.91	0.25	0.62	s	-1.01	0.22	0.55	s	-1.02	0.17	0.42	s
B11	-0.19	0.20	0.49		-0.53	0.25	0.64		-0.85	0.25	0.64	s	-0.95	0.19	0.47	s
B12	-0.07	0.21	0.51		-1.34	0.26	0.65	s	-1.95	0.25	0.62	s	-1.46	0.18	0.46	s
B15	-0.22	0.07	0.18	s	-0.80	0.13	0.33	s	-0.62	0.15	0.38	s	-1.03	0.10	0.25	s
B16	0.06	0.16	0.40		-0.77	0.21	0.51	s	-0.78	0.19	0.48	s	-0.56	0.14	0.36	s
B17	-0.14	0.20	0.50		-0.53	0.25	0.62		-0.55	0.22	0.55		-0.33	0.17	0.42	
B18	-0.20	0.20	0.49		-0.63	0.25	0.64		-0.68	0.25	0.62	s	-0.71	0.18	0.46	s
B19	0.12	0.19	0.47		-0.68	0.16	0.41	s	-0.76	0.15	0.38	s				
B20	-0.15	0.18	0.45		-0.60	0.21	0.53	s	-0.99	0.19	0.48	s	-0.79	0.15	0.37	s
B21	0.12	0.19	0.47													

Fisher test, differences in the height of the points to the previous and to the zero stage were created according to equation (10). These differences are due to the vertical movement of the observed points located on the construction object between stages $t^{(i)}$ and $t^{(i+1)}$. The results of the stability analysis of the observed points stabilized on the ground floor of the monolithic building according to equations (11–14) are monitored for the previous stage (Tab. 3) and the zero stage (Tab. 4). Statistically significant vertical movements of the observed points according to equation (13) are presented by the symbol in the "sig" column "s".

6. Discussion

Determination of the significance of height changes based on comparison with t times the variance of the height difference was carried out between neighbouring stages (Tab. 3) and to the zero stage (Tab. 4). The significance of the height changes at the observed points is a consequence of the real movement of the point and the symbol "s" has been indicated. But if it is a movement caused only as a result of the accumulation of measurement errors, then no symbol was given. When analysing the height changes of the adjacent stages, it is evident (Tab. 3) that the building usually decreases during the monitored period:

- between stages 0–1 there is a significant height change at 3 observed points (B2, B10 and B15), the average height change is $\overline{\Delta\hat{h}_{B_{i,j}}^{(01)}} = -0.12$ mm, the maximum drop is at the point $\Delta\hat{h}_{B_{10}}^{(01)} = -0.54$ mm, the minimum drop is a point rise $\Delta\hat{h}_{B_9}^{(01)} = -0.15$ mm, while positive values are at 4 observed points (B9, B16, B19 and B21).
- between stages 1–2 there is no significant height change at 2 observed points (B11 and B17), the average height change is $\overline{\Delta\hat{h}_{B_{i,j}}^{(12)}} = -0.71$ mm, the maximum drop is at the point $\Delta\hat{h}_{B_{12}}^{(12)} = -1.34$ mm, the minimum drop is at the point $\Delta\hat{h}_{B_{17}}^{(12)} = -0.53$ mm, while the same decreases were also observed at the

other 2 observed points (B9 and B11).

- between stages 2–3 there is no significant height change at 2 observed points (B5 and B17), the average height change is $\overline{\Delta\hat{h}_{B_{i,j}}^{(23)}} = -0.81$ mm, the maximum drop is at the point $\Delta\hat{h}_{B_{12}}^{(23)} = -1.95$ mm, and the minimum drop is at the point $\Delta\hat{h}_{B_3}^{(23)} = -0.48$ mm.
- between stages 3–4 there is no significant height change at 1 observed point (B17), the average height change is $\overline{\Delta\hat{h}_{B_{i,j}}^{(34)}} = -0.76$ mm, the maximum drop is at the point $\Delta\hat{h}_{B_{12}}^{(34)} = -1.46$ mm, and the minimum drop is at the point $\Delta\hat{h}_{B_{17}}^{(34)} = -0.33$ mm.

The single point B17 remained non-significant in all interstage analyses of height changes. When analysing the significance of height changes to the zero stage of the geodetic measurement, the drops between the individual stages were accumulated, so there is much less assumption that any point remained stable, or has significant height changes:

- between stages 0-2 there is no significant height change at 1 observed point (B9), the average height change is $\overline{\Delta\hat{h}_{B_{i,j}}^{(02)}} = -0.84$ mm, the maximum drop is at the point $\Delta\hat{h}_{B_{10}}^{(02)} = -1.45$ mm, the minimum drop is at the point $\Delta\hat{h}_{B_9}^{(02)} = -0.38$ mm.
- between stages 0-3 there is a significant height change at all observed points, the average height change is $\overline{\Delta\hat{h}_{B_{i,j}}^{(03)}} = -1.65$ mm, the maximum drop is at the point $\Delta\hat{h}_{B_{12}}^{(03)} = -3.36$ mm, and the minimum drop is at the point $\Delta\hat{h}_{B_9}^{(03)} = -1.17$ mm.
- between stages 0-4 there is also a significant height change at all observed points, the average height change is $\overline{\Delta\hat{h}_{B_{i,j}}^{(04)}} = -2.44$ mm, the maximum drop is at the point $\Delta\hat{h}_{B_{12}}^{(04)} = -4.82$ mm, and the minimum drop is at the point $\Delta\hat{h}_{B_{17}}^{(04)} = -1.55$ mm.

Based on the results of observing the significance between the mentioned stages, it was found that the B12 point with

Tab. 4. Verifications of the stability of the observed points based on the 0th stage

Tab. 4. Weryfikacja stabilności obserwowanych punktów na podstawie etapu 0

Point	Measur. stages 0-2 2016/03 - 2017/07				Measur. stages 0-3 2016/03 - 2018/06				Measur. stages 0-4 2016/03 - 2019/05			
	$\hat{dh}^{(02)}$	$\sigma_{dh}^{(02)}$	$dh_{krit}^{(02)}$	sig	$\hat{dh}^{(03)}$	$\sigma_{dh}^{(03)}$	$dh_{krit}^{(03)}$	sig	$\hat{dh}^{(04)}$	$\sigma_{dh}^{(04)}$	$dh_{krit}^{(04)}$	sig
	[mm]	[mm]	[mm]		[mm]	[mm]	[mm]		[mm]	[mm]	[mm]	
Reference points:												
194	-2.80*	0.10	0.25	s	-2.76*	0.08	0.21	s	-2.80*	0.09	0.23	s
195	-0.09	0.06	0.15		-0.15	0.07	0.17		-0.19	0.06	0.15	s
5001	0.12	0.06	0.15		0.18	0.05	0.13	s	0.20	0.03	0.08	s
Observed points:												
B2	-1.03	0.12	0.30	s	-1.85	0.09	0.24	s	-2.49	0.09	0.22	s
B3	-0.86	0.15	0.38	s	-1.34	0.13	0.32	s	-2.10	0.12	0.29	s
B4	-0.70	0.18	0.45	s	-1.21	0.16	0.39	s	-1.92	0.13	0.32	s
B5	-0.89	0.20	0.49	s	-1.43	0.17	0.43	s	-2.04	0.13	0.34	s
B6	-0.82	0.20	0.49	s	-1.60	0.17	0.43	s	-2.20	0.13	0.33	s
B7	-0.83	0.16	0.41	s	-1.61	0.14	0.36	s				
B8	-0.70	0.15	0.37	s	-1.55	0.12	0.31	s	-2.19	0.10	0.25	s
B9	-0.38	0.17	0.43		-1.17	0.14	0.36	s	-1.74	0.11	0.28	s
B10	-1.45	0.19	0.48	s	-2.46	0.17	0.42	s	-3.48	0.13	0.32	s
B11	-0.72	0.21	0.54	s	-1.57	0.20	0.49	s	-2.52	0.13	0.32	s
B12	-1.41	0.21	0.54	s	-3.36	0.19	0.47	s	-4.82	0.14	0.34	s
B15	-1.02	0.13	0.33	s	-1.64	0.10	0.26	s	-2.67	0.06	0.16	s
B16	-0.71	0.17	0.43	s	-1.49	0.14	0.36	s	-2.05	0.11	0.28	s
B17	-0.67	0.19	0.48	s	-1.22	0.17	0.42	s	-1.55	0.13	0.32	s
B18	-0.84	0.21	0.54	s	-1.52	0.19	0.47	s	-2.23	0.14	0.34	s
B19	-0.56	0.19	0.48	s	-1.32	0.17	0.44	s				
B20	-0.75	0.18	0.45	s	-1.74	0.16	0.39	s	-2.53	0.13	0.33	s

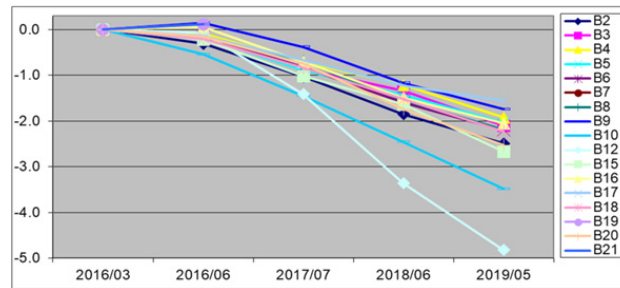


Fig. 6. Graphic presentation of the development of height changes of all observed points
 Rys. 6. Graficzna prezentacja rozwoju zmian wysokości wszystkich obserwowanych punktów

the biggest decline was not the "winner" right from the start of the tracking, but only after it overtook the B10 point in the decline. The height changes of the observed points in the form of a decline time series (Fig. 6) of a monolithic building in 1D show that the entire building descends approximately evenly.

It is also clear from the visualization that the observed points have a uniform decrease in the interval of 1 mm, except for two points that have a more pronounced tendency to decrease over the entire observed period than was presented from the numerical values. Height changes were also plotted in the floor plan of the monolithic building in the form of isolines of subsidence, to determine their surface distribution. According to the designer, the network of observed points is not evenly distributed, and the graphic visualization of subsidence in the form of isolines can be significantly distorted. The biggest drops (Fig. 7) are to the right of the central part (around B10) and in the right part in the strip of dense isolines is a decrease from the junction B6-B18 there to the junction B12-B20.

Even the drops to the zero stage (Fig. 8), presented using isolines, are the same, that the biggest drops are to the right of the central part, which has a smaller slope than at the right edge of the monolithic structure.

Based on the above findings, it is necessary to continue monitoring the building with repeated geodetic measurements in the next period to monitor the further development of the vertical

movements of the observed points of the monolithic structure, especially in the parts where the most significant decreases occur.

7. Conclusion

The measurement of displacements of building objects is constantly increasing because the available land with suitable foundation soils for construction within urban areas is decreasing and the construction of more complex buildings and architectural structures is progressing. These measurements make it possible to monitor the behaviour of the objects and to prevent various degrees of dysfunctionality or destruction, which can have catastrophic consequences. The aim of this article was to monitor the stability of a monolithic building by measuring its height using a Leica DNA03 digital levelling instrument. The measured elevations met the accuracy criteria imposed on such measurements, and based on them, height estimates of the observed points were determined at different stages with their corresponding accuracy. Subsequently, significant height differences between neighbouring stages and relative to the zero stage of levelling measurements were determined. The height changes of the observed points presented in the overview tables show that the most significant changes in height, compared to the zero stage, were observed at two points: B10 with a value of -3.48 mm and B12 with -4.82 mm., The average height changes from the last three



Fig. 7. Graphical visualization of height changes between neighbouring stages of geodetic measurement
 Rys. 7. Graficzna wizualizacja zmian wysokości pomiędzy sąsiednimi etapami pomiaru geodezyjnego

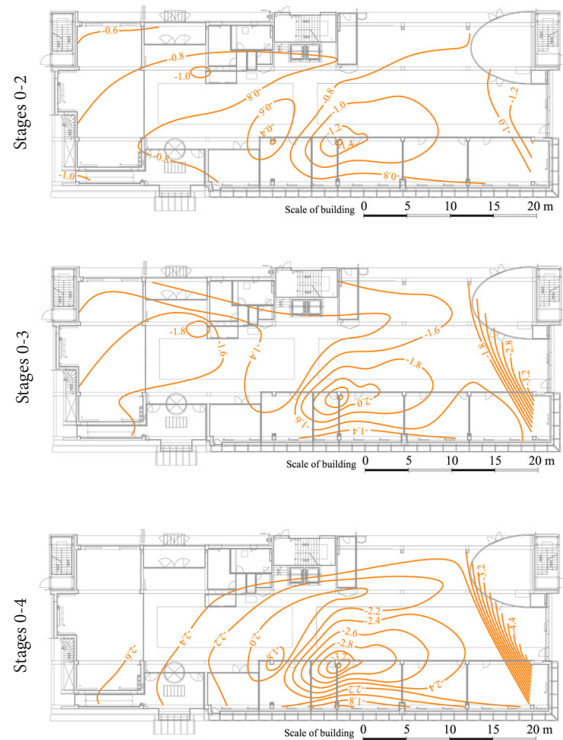


Fig. 8. Graphical visualization of height changes to the zero stage of geodetic measurement
 Rys. 8. Graficzna wizualizacja zmian wysokości do zerowego stopnia pomiaru geodezyjnego

stages of monitoring were -0.76 mm. These height changes were plotted as a 1D grouped time series and as 2D isolines on the building floor plan to visualize the magnitude of these changes. However, due to the irregularity of the height point

net according to the designer's intentions, and the fact that some observed points disappeared or were destroyed during construction, the graphical visualization may present significant results in a distorted manner.

Literatura – References

1. ABELOVIČ, J., MIČUDA, J., MITÁŠ, J., WEIGEL, J., Measurements in geodetic networks. Alfa, Bratislava, 1990, (in Slovak).
2. BOHM, J., SVOBODA, J. Geometric levelling. State publishing house of technical literature, Praha, 1960, (in Czech).
3. KLOBUŠIAK, M. Optimal software for processing measurements of horizontal and vertical displacements of water structures. Slovak surveyor and cartographer, 19(3), p. 8–14, 2014, ISSN 1335-4019.
4. KUCHAR, J., GOLUCH, P., CMIELEWSKI, K., RZEPKA, J., BUDZYN, G. A functional-precision analysis of the vertical comparator for the calibration of geodetic levelling systems. Measurement, 163(1), 107951, 2020, DOI: 10.1016/j.measurement.2020.107951.
5. LABANT, S., RÁKAY, S., GERGEOVA, M.B., LEICHER, L., SUSTEK, P. Vertical movements of tripods and their effect on the results of precise levelling measurements. Arabian Journal of Geosciences, 15(10), 980, 2022, DOI: 10.1007/s12517-022-09999-z.
6. MICHALČÁK, O., KOPÁČIK, A., LUKÁČ, Š., PÍŠ, D. Engineering geodesy: Selected engineering-geodetic methods. STU, Bratislava, 1995, (in Slovak).
7. MICHALČÁK, O., VOSIKA, O., VESELÝ, M., NOVÁK, Z. Engineering surveying I. Alfa, Bratislava, 1985, (in Slovak).
8. RÁKAY, Š., LABANT, S., BARTOŠ, K. Verification of floor planarity by trigonometrical measurement of heights on a 5-storey monolithic building. Geodesy and Cartography, 44(1), 14–21, 2018. <https://doi.org/10.3846/gac.2018.269>.
9. SABOVÁ, J., JAKUB, V. Geodetic deformation survey. Technical University of Košice, Košice, 2007, (in Slovak).
10. ŠUTTI, J. Surveying. Alfa, Bratislava, 1987, (in Slovak).
11. WITTE, B., SPARLA, P. Vermessungskunde und Grundlagen der Statistik für das Bauwesen. Wichmann, H., 2015.
12. Optics and optical instruments. ISO 17123-2:2001. Field procedures for testing geodetic and surveying instruments. Part 2: Levels., 1st ed., Geneva, 2001.
13. Guidelines for managing geodetic foundations. S 74.20.73.11.00. Geodesy, Cartography and Cadastre Authority of the Slovak Republic, Bratislava, 2006.
14. Measurement of deformation of building constructions. Slovak technical standard STS 73 0405. Slovak Office of Standards, Metrology and Testing, Bratislava, 2022, (in Slovak).
15. State levelling network. Geodesy, Cartography and Cadastre Authority of the Slovak Republic. [online]. [access: 2024-01-09]. <https://www.geoportalsk.sk/sk/geodeticke-zaklady/body-gz-a-geodeticke-siete/statna-nivelacna-siet/>.
16. University Science Park Technicom. Technical University of Košice. [online]. [access: 2023-12-04]. <https://uvptech-nicom.sk/uvp-technicom-faza-i/>.

Analiza stabilności wysokości punktów obiektu o konstrukcji monolitycznej

Pomiary geodezyjne mają na celu monitorowanie zachowania obiektów i zapobieganie różnym stopniom ich niefunkcjonalności lub zniszczeniu. Mierząc przemieszczenia pionowe, monitoruje się stabilność wysokości budynku monolitycznego w odniesieniu do poprzednich etapów pomiaru. Pomiary przeprowadzono przy użyciu niwelatora cyfrowego Leica DNA03 oraz pasek kodowych invar GPCL2 o długości 2 m. Punkty obiektu stabilizowano głównie w konstrukcji nośnej budynku, lecz w miejscach problematycznych konieczna była także stabilizacja w stropie. Punkty obiektowe w suficie mierzono za pomocą specjalnego metalowego uchwytu do zawieszania łat poziomujących. Po wstępnej weryfikacji zmierzonych wysokości i tego, czy spełniają one kryteria dokładności, następuje obróbka, po której następuje zastosowanie modelu Gaussa-Markowa opartego na metodzie poprawek najmniejszych kwadratów. Oszacowania nieznanych parametrów z pomiarów etapowych posłużyły do obliczenia różnic wysokości obserwowanych punktów, które charakteryzują zachowanie obiektu monolitycznego. Znaczące zmiany wysokości wykryto na podstawie dokładności szacowanych wysokości, określając, czy reprezentują one znaczne spadki, czy po prostu kumulację błędów pomiarowych. Zmiany wysokości punktów obiektu zwizualizowano graficznie w 1D jako szeregi czasowe spadku oraz w 2D jako izolinie przemieszczeń pionowych na podstawie planu piętra monolitycznego budynku.

Słowa kluczowe: konstrukcja monolityczna, poziomowanie, monitorowanie stateczności, zmiany wysokości, izolinie ruchów